

DOE/ET-53088-322

IFSR #322

**Self-Similar Evolution of Nonlinear
Magnetic Buoyancy Instability**

K. Shibata,^(a) *T. Tajima*
Institute for Fusion Studies
The University of Texas at Austin
Austin, Texas 78712

and
R. Matsumoto
Department of Astronomy
University of Kyoto
Kyoto 606, Japan

June 1988

^(a) Dept. of Earth Sciences, Aichi University of Education, Aichi, Japan

Self-Similar Evolution of Nonlinear Magnetic Buoyancy Instability

K. Shibata^(a) and T. Tajima

Institute for Fusion Studies,
University of Texas, Austin, TX 78712

and

R. Matsumoto

Department of Astronomy, University of Kyoto,
Kyoto 606, Japan

received 2 May 1988

A new type of self-similar solution of ideal magnetohydrodynamics in the nonlinear stage of undular mode ($\mathbf{k} \parallel \mathbf{B}$) of magnetic buoyancy instability (Parker instability or ballooning instability) is found through MHD simulation and theory. The solution has the characteristics of nonlinear instability in Lagrangian coordinates; the fluid velocity and the Alfvén speed on each magnetic loop increases exponentially with time, because the loop is evacuated by the field aligned motion of matter due to gravitational acceleration.

PACS numbers: 52.35.Py, 52.65.+z, 96.60.Hv

A plasma that is supported by a magnetic field under the gravitation is known to be subject to the Kruskal-Schwartzschild (or magnetic Rayleigh-Taylor) instability.¹ Similar instability results in a gravitationally stratified plasma with non-uniform magnetic field, called magnetic buoyancy instability.² The magnetic curvature can play a role similar to gravity. The undular mode ($\mathbf{k} \parallel \mathbf{B}$) of the magnetic buoyancy instability, where \mathbf{k} and \mathbf{B} are the wavenumber and magnetic field vectors, is believed to be important in various physical phenomena ranging from astrophysical plasmas² to fusion plasmas,³ because this mode can be unstable even when the plasma layer is stable against the interchange mode ($\mathbf{k} \perp \mathbf{B}$). For example, for an isothermal case the former is unstable when $dB/dz < 0$, while the latter is unstable only when $d/dz(B/\rho) < 0$, where ρ is the density and the gravitation is in the negative z direction. Parker⁴ applied the undular instability to the disk of Galaxy. Hence, this instability is called the Parker instability in some astrophysical literatures. The ballooning instability⁵ in fusion plasmas has essentially the same physical characteristics as that of the Parker instability with general orientation of \mathbf{k} with respect to \mathbf{B} . In spite of many linear theory investigations, however, the physics of nonlinear stages of this instability is much less known. In this letter, we report the discovery of a self-similar solution in the nonlinear stage of the undular instability, which has a characteristics of the *nonlinear instability* (exponential growth in time) in a Lagrangian frame.

A self-similar solution has been found by using nonlinear simulations,⁶

which are carried out with assumptions that (1) two-dimension (2D) [$V_y = B_y = \partial/\partial y = 0$ in Cartesian coordinate (x, y, z)], (2) ideal magnetohydrodynamics, (3) a constant gravitational acceleration (g) in the negative z -direction. A full set of compressible ideal MHD equations with the adiabatic index γ ($=1.05$) are solved by using modified Lax-Wendroff scheme with artificial viscosity. The initial gas layer is in magneto-static equilibrium and consists of a cold isothermal plasma layer, which is partly permeated by horizontal isolated magnetic flux sheet in $z_0 < z < z_0 + D$, and a hot isothermal, non-magnetized plasma layer above the cold layer. Hereafter, the units of length, velocity, and time are H , C_s , and H/C_s , where $H = C_s^2/(\gamma g)$ is the scale height and C_s is the sound speed in the cold layer. We have taken $\beta = 1$, where β is the ratio of magnetic to gas pressure in the magnetic sheet. We assume periodic boundary for $x = 0$ and X_{max} , conducting wall boundary for $z = 0$, and free boundary for $z = Z_{max}$. With $k_y = 0$, the plasma layer is unstable for the long wavelength [$\lambda (= 2\pi/k_x) > \lambda_c$] perturbation, and the critical wavelength [$\lambda_c \simeq 4\pi H/(1 + 2/\beta)^{1/2}$ if $D = \infty$ and $\gamma = 1$]² and the most unstable wavelength are $\simeq 14H$ and $\simeq 20H$, respectively, for $\beta \simeq 1$ in our magnetic flux sheet with $D = 4$.⁶ The linear theoretical growth rate for $\lambda = 20H$ is $0.121 C_s/H$. [The growth rate for $D = \infty$ and $\gamma = 1$ is about $0.3(1 + 2/\beta)^{-1} V_A/H = 0.3(2/\beta)^{1/2}(1 + 2/\beta)^{-1} C_s/H$ when $0.5 < \beta < \infty$.]² We initially give the system small-amplitude perturbations ($V_{max} = 0.01 C_s$) having the same spatial distributions as those of linear

eigenfunctions in the unstable mode with $\lambda = 20H$ in the finite horizontal domain ($X_{max}/2 - \lambda/2 < x < X_{max}/2 + \lambda/2$).

Fig. 1 shows the time evolution of magnetic lines of force, the velocity field, and the density distribution. As the magnetic loop rises, the gas slides down along the loop. Spikes of dense regions are created on the valleys of the undulating field lines, whereas the rarefied regions are produced around the top of magnetic loops. The most significant character in the nonlinear stage ($t > 40$) is the approximate *self-similar pattern* of magnetic loop expansion; the rise velocity of the magnetic loop and the velocity of downflow along the loop increase with height as the loop expands and ascends. Fig. 2 shows some physical quantities at $x = X_{max}/2$ (midpoint of the magnetic loops), indicating approximate self-similar behavior as a function of height. We also find

$$V_z = a_1 z; \quad V_A = a_2 z, \quad (1)$$

where $a_1 \simeq 0.06$ (for $t < 60$), $a_2 \simeq 0.3$, and z is the height measured from $z_0 (= 4)$. On the other hand, we find the density and magnetic field strength have the power-law distribution;

$$\rho \propto z^{-4}; \quad B_x \propto z^{-1}. \quad (2)$$

We shall now look for a self-similar solution of the problem by analytical method. We have the following relation from Eq. (1); $\partial V_z / \partial \tau = \partial V_z / \partial t + V_z \partial V_z / \partial z = a_1 V_z$, where τ is the time in Lagrangian coordinates, while t and

z are the Eulerian coordinates. This leads to

$$V_z(\xi, \tau) = a_1 \xi \exp(a_1 \tau), \quad (3)$$

where $\xi = z \exp(-a_1 \tau)$ is the Lagrangian coordinate.

We assume the quasi one-dimension (1D) for the problem, i.e. we consider only vertical (z) variation of the physical quantities at the midpoint of the loop. The basic equations of our quasi-1D problem are

$$\partial \rho / \partial t = -\partial(\rho V_z) / \partial z - \partial(\rho V_x) / \partial x, \quad (4)$$

$$\rho(\partial V_z / \partial t + V_z \partial V_z / \partial z) = -[\partial(B_x^2 / 8\pi) / \partial z + B_x^2 / 4\pi R], \quad (5)$$

$$\partial B_x / \partial t = -\partial(B_x V_z) / \partial z, \quad (6)$$

where R is the radius of curvature of field lines at the midpoint of the magnetic loop. The last term on the right hand side of Eq. (5) is in a simplified phenomenological form in order to keep the variation in one (z) direction. Here we neglect the gas pressure and the gravitational forces in Eq. (5), and the reason will become clear after the self-similar solutions are found. The neglect of B_z -related term in Eq. (6) may be justified because $B_z \ll B_x$ near the midpoint of the magnetic loop. A central Ansatz of the present quasi-1D model is

$$\partial(\rho V_x) / \partial x = (N - 1) \partial(\rho V_z) / \partial z, \quad (7)$$

where N is assumed to be constant. The left hand term in Eq. (7) corresponds to fluid leaking along the field line away from the midsection of the

loop because the bent loop allows the fluid to escape under the gravitational influence. Here, we measure the amount of matter leakage in the horizontal direction in terms of the vertical flow motion. If $N = 1$, no leakage arises, which corresponds to a pure 1D motion. In order to have matter leakage, $N < 1$. $N - 1$ is a parameter that measures severity of matter leakage in the x -direction. We further assume $R = cz$ and $c = \text{constant}$, which is a manifestation of the self-similar evolution of the spatial pattern of the loop, as observed in Fig. 1(c).

Under these assumptions, a particular self-similar solution, that satisfies our empirical velocity functions (1) and (3) and quasi-1D MHD equations (4)–(6), is found;

$$\rho = r_1 \xi^{-4-2q} \exp(-4a_1 \tau) = r_1 z^{-4-2q} \exp(2qa_1 t), \quad (8)$$

$$B_x = b_1 \xi^{-1-q} \exp(-a_1 \tau) = b_1 z^{-1-q} \exp(qa_1 t), \quad (9)$$

where $q = 3N/[2(1 - N)]$, $r_1 = r(\xi = 1)$, $b_1 = a_1 [4\pi r_1 / (q + 1 - 1/c)]^{1/2}$. The simulation results (2) [see Figs. 2 (c) and (d)] indicate the analytical solution with $N = q = 0$, which leads to a steady solution in Eulerian coordinates in Eqs. (8) – (9). Our self-similar solution leads to $\rho g / [\partial/\partial z (B_x^2/8\pi)] \propto z^{-1}$ and $\partial p/\partial z / [\partial/\partial z (B_x^2/8\pi)] \simeq (C_s/V_A)^2 \propto z^{-2}$. Hence, as the magnetic loop rises, both forces decrease more rapidly than the magnetic force; as long as above force ratios are less than unity at $t = 0$, the neglect of the gravitational and the gas pressure forces in the nonlinear evolution is valid, while the nonlinear

growth rate a_1 is found to be related g (see below).

Fig. 3 shows the time evolution of the Lagrangian displacement of a test particle at the midpoint of the loop in the simulation results. In the initial stage, the growth rate of the perturbation amplitude agrees well with linear theoretical values ($\omega_l = 0.121$). The amplitude increases exponentially with time even in the nonlinear stage ($t > 40$), and the growth rate also agrees with theoretical values; $z \propto \exp(\omega_n t)$ and $\omega_n \simeq a_1 \simeq 0.06 \simeq \omega_l/2$.

More general analysis⁶ shows that Eqs. (4) – (7) have several self-similar solutions with power-law time dependence under the boundary condition $V_z(z = 0) = 0$, which are summarized in Table 1. One solution (for $N = 2/(3\alpha) \ll 1$) has the characteristics that $V_z \propto z/t$, $\rho \propto z^{-4}$, $B_x \propto z^{-1}$, and explains the behavior of simulation results after $t > 60$ in Fig. 2 (a); after the magnetic loop enters the hot layer.

It is known that the rise velocity V_b of the bubble observed in the laboratory⁷ and in the ionosphere⁸ tend to be steady in the Lagrangian frame and is in proportion to the radius R_b of the bubble; $V_b = a_3 R_b$, where $a_3 \simeq (1/3 - 1/2) \times (g/R_b)^{1/2}$ is of the order of the linear growth rate of the Rayleigh-Taylor instability. This is similar to our results that $V_z = a_1 z \simeq a_1 R$, where R is the curvature radius of the magnetic loop, $a_1 \simeq \omega_l/2$ and ω_l is the linear growth rate. However, the rise velocity of our magnetic loop is not steady in the Lagrangian frame, but increases exponentially with time. This *nonlinear instability* in the Lagrangian frame is also observed in the exact solution

found by Ott⁹ for the Rayleigh-Taylor instability of a thin, cold gas layer, which is supported against gravity by a hot gas, with a second hot gas above the thin layer. In this case, the growth rate in the nonlinear stage is exactly the same as that in the linear stage. Physically, this is because cold gas in the thin layer freely falls along the curved interface between two hot gases, and mathematically, because the nonlinear basic equations become linear ones in the Lagrangian frame.¹⁰ Although the nonlinear growth rate is not exactly equal to the linear growth rate in our case, the involved physics is common between ours and Ott's problem; the exponential growth in the nonlinear stage is due to the gravitational free fall *along* the magnetic loop. That is, the equation of motion along magnetic loop in our problem is written as $d^2\theta/dt^2 = (g/R)\theta$, where $\theta = x/R$ and x is the horizontal distance from the midpoint of the loop.⁶ This equation has the exponential solution with the growth rate of $(g/R)^{1/2}$. In addition to this character of *nonlinear instability*, our solution has the *self-similar* property, which is not in Ott's solution.

The authors thank Drs. W. Horton, J. van Dam, R. Steinolfson, R. Rosner, M. Nambu, for useful discussions. Computations are performed on FACOM VP200 at the Institute of Plasma Physics, Nagoya University. This work is supported by NSF, NASA and USDOE.

(a) Permanent address: Department of Earth Sciences, Aichi University of Education, Kariya, Aichi 448, Japan

¹ M. D. Kruskal and M. Schwarzschild, Proc. Roy. Soc. London **223A**,

348 (1954).

² E. R. Priest, *Solar Magnetohydrodynamics* (Dordrecht: Reidel, 1982), p. 293; E. N. Parker, *Cosmical Magnetic Field* (Oxford: Clarendon Press, 1979), p. 314.

³ W. A. Newcomb, *Phys. Fluids* **4**, 391 (1961).

⁴ E. N. Parker, *Astrophys. J.* **145**, 811 (1966).

⁵ B. Coppi and M. N. Rosenbluth, in *Plasma Phys. and Cont. Nucl. Fus. Res. vol. 1*, (IAEA, Vienna, 1966), p. 617.

⁶ K. Shibata, T. Tajima, R. Matsumoto, T. Horiuchi, T. Hanawa, R. Rosner, and Y. Uchida, *Astrophys. J.* to be submitted (1988).

⁷ R. M. Davies and G. I. Taylor, *Proc. Roy. Soc. London*, **A200**, 375 (1950).

⁸ e.g. S. L. Ossakow and P. K. Chatuvedi, *J. Geophys. Res.* **83**, 2085 (1978).

⁹ E. Ott, *Phys. Rev. Lett.* **29**, 1429 (1972).

¹⁰ J. M. Dawson, *Phys. Rev.* **113**, 383 (1959).

Figure Captions

Fig. 1 Simulations results; (a) the magnetic field lines $\mathbf{B} = (B_x, B_z)$, (b) the velocity vector $\mathbf{V} = (V_x, V_z)$, (c) density contours ($\log \rho$).

Fig. 2 The distributions in z of (a) the vertical velocity V_z , (b) the local Alfven speed V_A , (c) the horizontal magnetic field ($\log B_x$), (d) the density ($\log \rho$) at $x = X_{\max}/2 = 40$. The numbers attached to the curves correspond to the following time (in unit of H/C_s); (1) $t = 42.1$, (2) 49.6, (3) 57.6, (4) 64.6.

Fig. 3 The time evolution of Lagrangian displacement ($\Delta z_m = z_m(t) - z_m(0)$; solid curve) of a test particle. The dashed line shows the linear growth with $\omega_l = 0.121 C_s/H$, and the dash-dotted line shows the nonlinear growth with $\omega_n = 0.06 C_s/H$.

Table 1 Summary of Self-Similar Solutions

$Z\ddot{Z}/\dot{Z}^2 \neq 1$ $[Z \propto \tau^\alpha]$	$\delta \neq 1$	$N \neq 0$	no solution
		$N = 0$	$B_x \propto \tau^{-\delta/(1-\delta)} \zeta^{-\delta} \propto z^{-\delta}; \alpha = 1/(1-\delta)$
	$\delta = 1$	$N \neq 1$	$B_x \propto \tau^{-\alpha} \zeta^{-1-h} \propto t^{-h\alpha} z^{-1-h}$ where $h = (3N - 2/\alpha)/[2(1 - N)]$
		$N = 1$	$B_x \propto \tau^{-\frac{2}{3}} \zeta^{\frac{1}{2}-\frac{1}{\epsilon}} \propto t^{-1+\frac{2}{3\epsilon}} z^{\frac{1}{2}-\frac{1}{\epsilon}}; \alpha = 2/3$
$Z\ddot{Z}/\dot{Z}^2 = 1$ $[Z \propto \exp(a_1 \tau)]$	$\delta \neq 1$	any N	no solution
	$\delta = 1$	$N \neq 1$	$B_x \propto \zeta^{-1-q} \exp(-a_1 \tau) \propto z^{-1-q} \exp(qa_1 t)$ where $q = 3N/[2(1 - N)]$
		$N = 1$	no solution

Note: $\zeta = z/Z(\tau)$ is Lagrangian coordinate, z is Eulerian coordinate (height measured from the base of the initial magnetic flux tube), and δ is the exponent of velocity function ($V_z \propto z^\delta$).

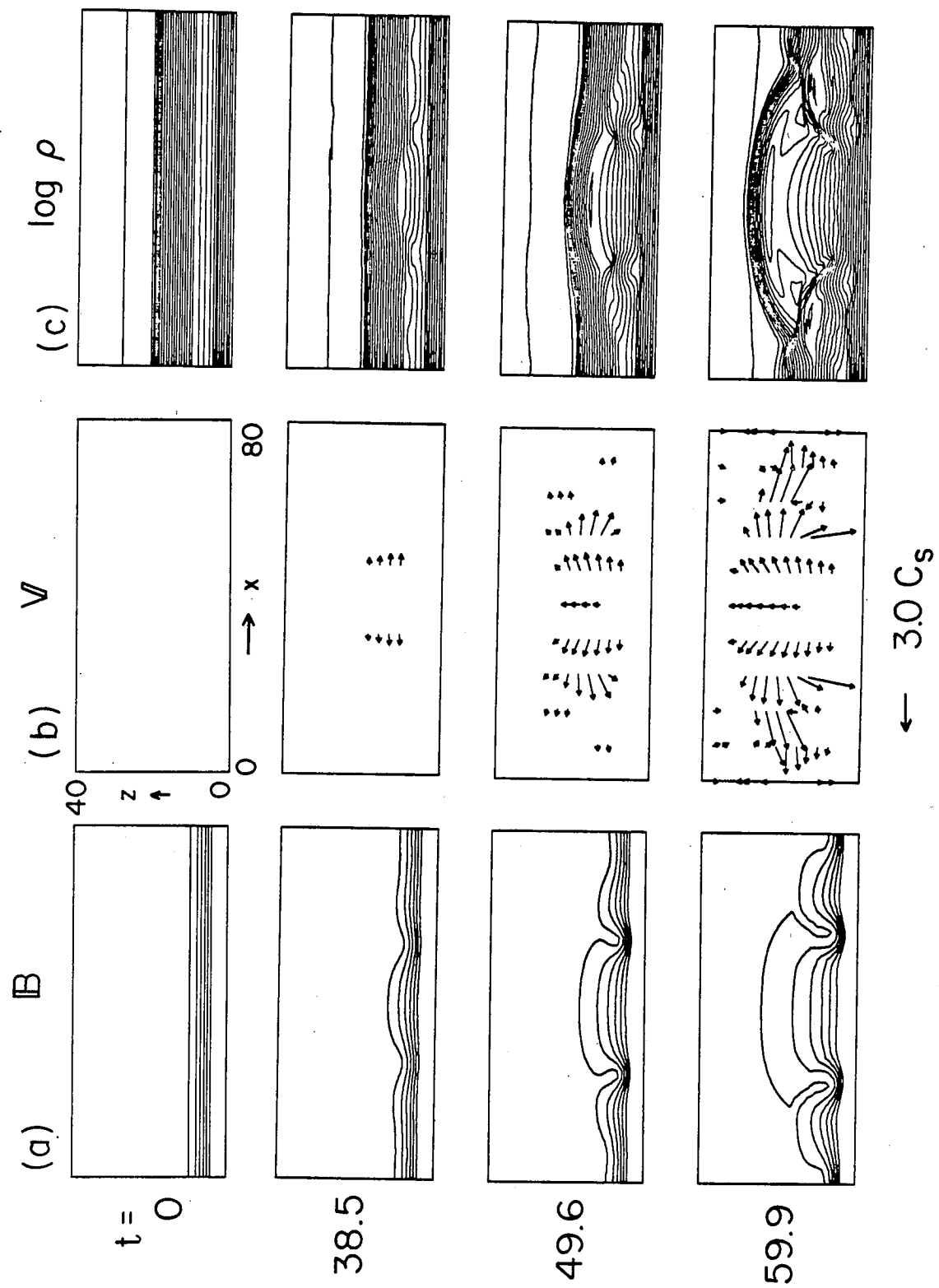


Fig. 1

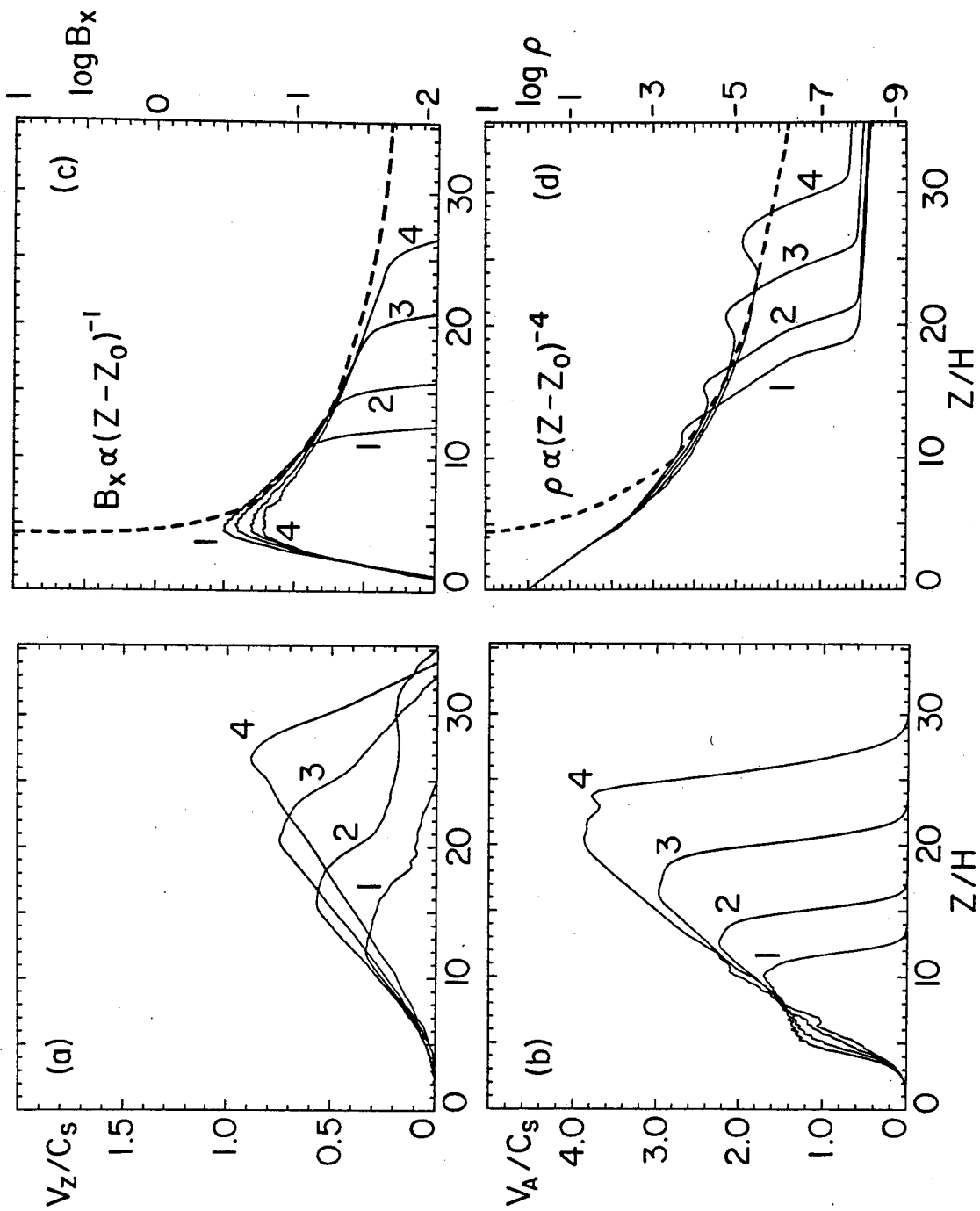


Fig. 2

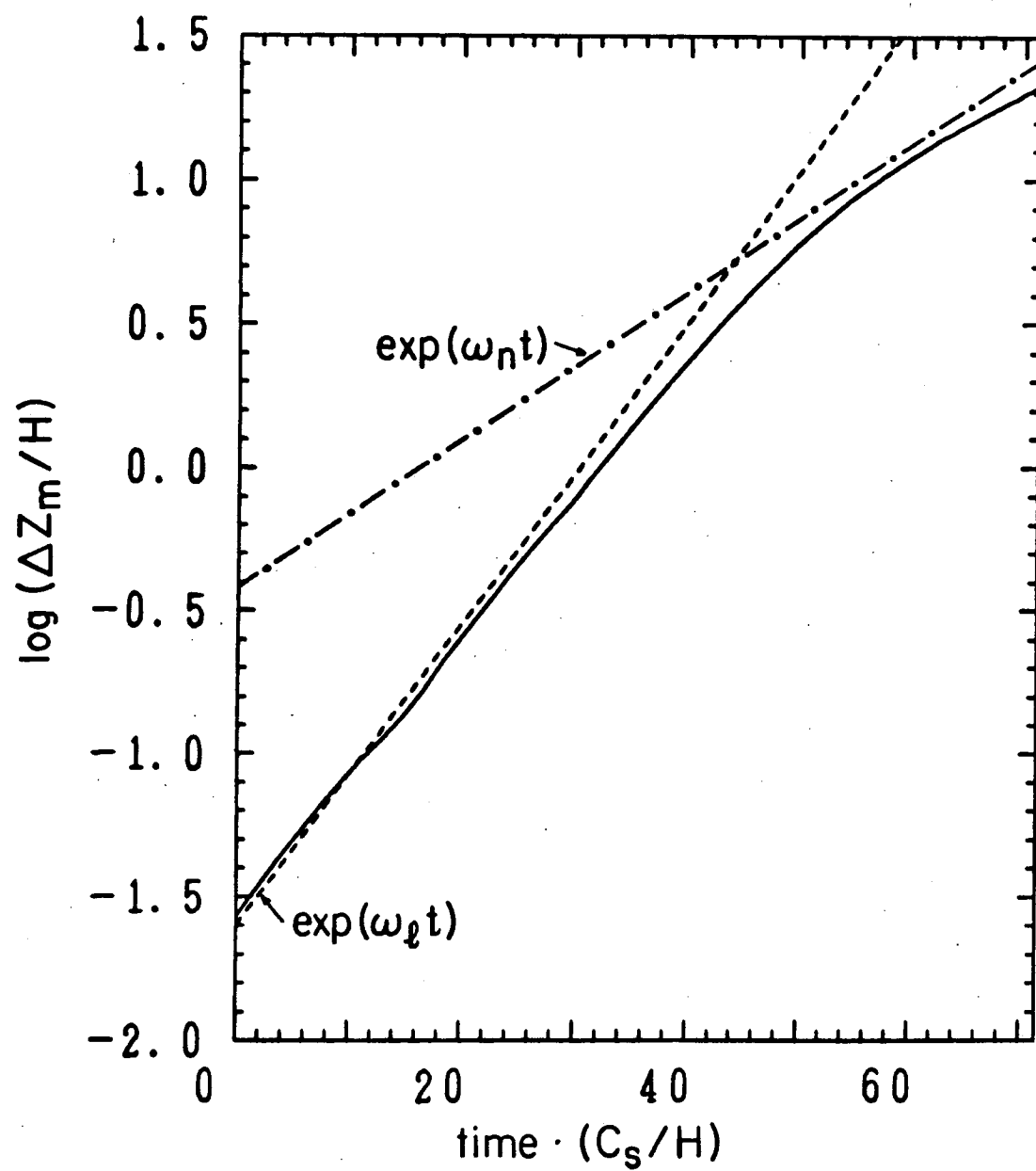


Fig. 3